HiSST: 2nd International Conference on
High-Speed Vehicle Science Technology
11–15 September 2022, Bruges, Belgium

Validation of Internal Energy Coupling to Chemistry in Hypersonic Flow

Thomas E. Schwartzentruber[1], Maninder Grover[2], Erik Torres[3]

Abstract

Predictive simulations of the shock-heated, high-temperature environment that surrounds a hypersonic vehicle during flight is an important aspect of advancing hypersonic vehicle technology. It is not possible to reproduce flight conditions in ground-testing facilities and flight-testing is expensive. As a result, advanced aerodynamic and chemical kinetics modeling, combined with high performance computing, plays a critical role in advancing hypersonic flight science. Considerable recent effort has been devoted to understanding and modeling internal energy relaxation and dissociation in hypersonic flows using first-principles calculations. In the past ten years, 23 potential energy surfaces (PESs) that govern the collision dynamics of relevant air species (N_2, N, O_2, O, and NO) in the ground electronic state have been developed and used to simulate dissociating nitrogen and oxygen gas. These simulations have predicted the precise coupling between gas internal energy and chemical reactions including non-Boltzmann effects. Recent experimental measurements are now able to validate these non-Boltzmann coupling predictions for the first time.

Keywords: *Hypersonic flow, Reacting flow, Nonequilibrium flow*

1. Introduction

1.1. Thermochemical nonequilibrium in hypersonic flow

An object travelling at hypersonic speed through an atmosphere generates a strong shock wave that creates a thin region of high temperature gas surrounding vehicle surfaces. Understanding and predicting the extreme gas state in this thin 'shock-layer' region is important for thermal protection system (TPS) material selection and for predicting the material's response and possible failure. Due to the high flow speed, the shock-layer gas is often in a state of thermal nonequilibrium (where energy is not equally partitioned across translational, rotational, vibrational, and possibly electronic, energy modes) and is also in a state of chemical nonequilibrium. It is well established that the internal energy state of the gas and the rate of chemical reactions are strongly coupled [1,2]. For this reason, two-temperature models are used in computational fluid dynamics (CFD) simulations of hypersonic flow. For example, the most widely used model is the Park model [3] and a range of alternative multi-temperature models have been proposed, such as the Marrone Treanor model [4] and a recent modified version that is based on new first-principles quantum chemistry data, called the MMT model [5,6].

Such two-temperature models solve the compressible Navier-Stokes equations (mass, momentum, and energy transport equations with source terms for finite-rate chemistry species production/removal) and also solve an additional transport equation for the average vibrational energy of the gas. This enables prediction of thermal nonequilibrium between the translational/rotational modes and the vibrational mode, and therefore enables explicit coupling between the vibrational energy of the gas and chemical reaction rates. A primary effect is that the gas must first excite vibrationally before significant dissociation occurs [7]. Therefore, the characteristic relaxation time for the vibrational energy mode becomes an important parameter that influences the amount of dissociation that occurs in the thin

[1] *University of Minnesota, 110 Union St. SE, Minneapolis, MN, U.S.A., schwart@umn.edu*
[2] *University of Minnesota, 110 Union St. SE, Minneapolis, MN, U.S.A., etorres@umn.edu*
[3] *University of Dayton Research Institute, Dayton, OH, U.S.A., mgrover1@udayton.edu*

shock layer. It is well established that such two-temperature models more accurately capture the dissociation process behind strong shocks compared to models that assume thermal equilibrium and no internal energy coupling with chemistry.

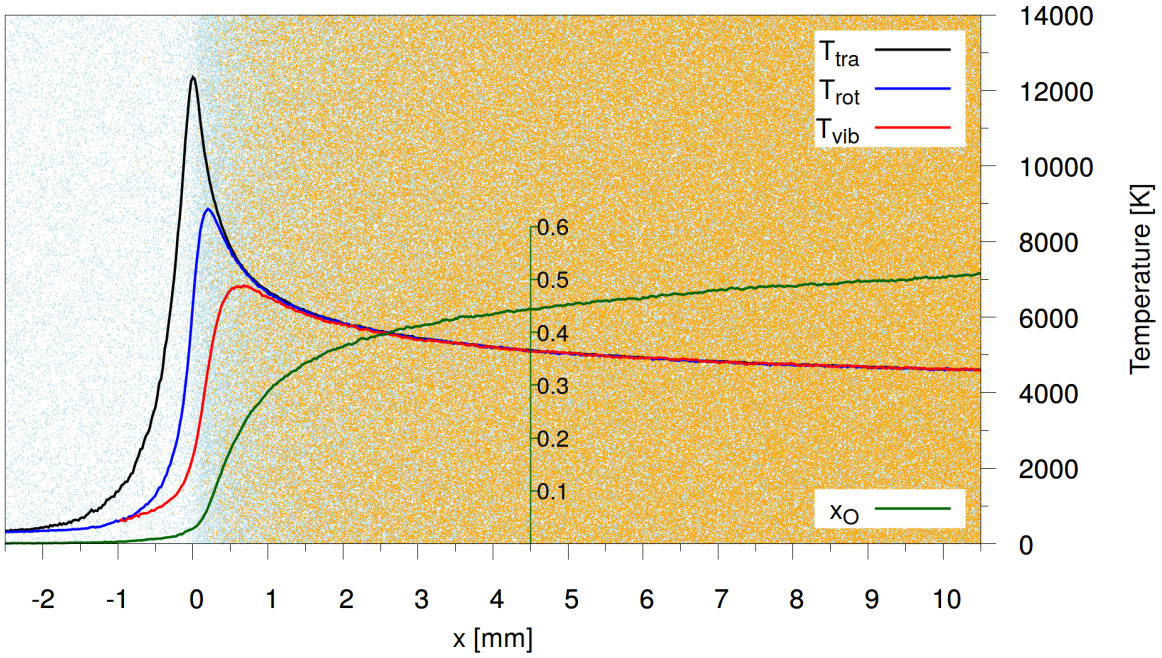

Fig 1. Direct molecular simulation (DMS) of a 4.4 km/s normal shock wave in oxygen. Simulation results were initially presented in Ref. [8].

An example simulation (using the Direct Molecular Simulation method described in section 1.3) of a 4.4 km/s normal shock wave in oxygen gas is shown in Fig. 1 [8]. Across the shock wave, first the translational temperature rapidly rises, followed quickly by the rotational temperature. The translational and rotational modes equilibrate with each other while the vibrational temperature increases at a slower rate, eventually equilibrating with the other modes. A key result, seen in Fig. 1, is that significant dissociation does not begin during the translational temperature spike, rather dissociation begins only after the vibrational temperature begins to excite. Due to the small length-scales involved, most experimental measurements are taken in the post-shock region where the gas appears to be close to thermal equilibrium yet continues to dissociate. This is called the Quasi-Steady-State (QSS) dissociating region (approximately $x > 2$ mm in Fig. 1).

1.2. Nonequilibrium (non-Boltzmann) internal energy distributions

Two-temperature models track the *average* vibrational energy of the gas. Under equilibrium conditions, only the average energy is required to define the equilibrium (Boltzmann) distribution of internal energy levels of molecules in the gas. However, under thermochemical nonequilibrium conditions the vibrational energy distribution may be non-Boltzmann. Since molecules in the upper vibrational energy states are exponentially more likely to dissociate, then the precise population distribution (any differences compared to a Boltzmann distribution) could lead to important macroscopic effects.

Multi-temperature models do not explicitly account for non-Boltzmann distributions. For this reason there has been extensive research to understand the full rotational-vibrational excitation process, including non-Boltzmann energy distributions, and their effects on chemical reactions [9-20]. Many of these studies involve first-principles calculations that have predicted the evolution of non-Boltzmann distributions in shock-heated gases. Master equation and state-to-state methods, that compute the evolution of all quantized rovibrational levels, have been used to study gas systems involving only atom-diatom processes (such as N-N_2 and O-O_2 collisions). However, these methods become intractable for gas systems that also involve diatom-diatom processes (such as N_2-N_2, O_2-O_2, and N_2-O_2 collisions) because there are far too many quantized rovibrational state transitions (approximately 10^{15} possible energy transitions for N_2-N_2 collisions). As a result, grouping or binning models must be employed.

Different modeling choices lead to different predictions, and such model development is currently an active area of research.

1.3. Direct Molecular Simulation (DMS) and Validation Challenges

For this reason, the Direct Molecular Simulation (DMS) method was developed [21,22], for which the sole model input is a set of potential energy surfaces (PESs) that dictate the forces between atoms (similar to molecular dynamics). The method was originally proposed by Koura [23], and was called Classical Trajectory Calculation – Direct simulation Monte Carlo (CTC-DSMC). The method has been extended to incorporate ab-initio potential energy surfaces (PESs), accommodate all manner of rovibrational relaxation processes, exchange reactions, and dissociation reactions, and can now accommodate large sets of PESs to simulate multispecies mixtures. Complete details of the method can be found in Ref. [22]. The DMS method maintains the accurate model assumptions of the DSMC method (free flight of particles for a fraction of the mean-collision-time, randomized impact parameters for collisions, and simulating only a fraction of real particles is required), but the method replaces stochastic DSMC collision *models* with classical trajectory calculations using a PES. The DMS method can also be viewed as an acceleration technique for molecular dynamics simulation of dilute gases. The DMS method has been used to simulate thermochemical nonequilibrium for air-relevant species under isothermal conditions [9,10,15,16], adiabatic conditions [13,17], 1D shock wave flows [8], and even 2D and 3D flows on large computer clusters [24]. The most recent results involve simulating dissociating 5-species air mixtures [25] in the ground-electronic state using 23 PESs developed in the Chemistry department at the University of Minnesota (PES subroutines are freely available on the POTLIB website [26]). Such DMS simulations (an example was shown in Fig. 1) predict the evolution of non-Boltzmann internal energy distributions where all energy transitions and chemical reactions resulting from the PESs are possible, with no binning/grouping models required.

DMS studies have quantified non-Boltzmann effects and their coupling to chemical reactions. The problem is, to date, there have been no experimental measurements with sufficient accuracy to validate these non-Boltzmann predictions. Even the best optical diagnostics can only measure vibrational states up to, approximately, the tenth quantum level in relevant high enthalpy flows. The population of higher levels generated in hypersonic flow facilities is simply too low to obtain sufficient signal. Due to the exponential coupling between vibrational energy and dissociation, it is the highest vibrational levels (even with low populations) that have a noticeable effect on the dissociation process.

Recently, a new set of experiments for $O+O_2$ and O_2+O_2 dissociation rates were performed at Stanford university [27], where measurement uncertainty was much lower than for previous measurements reported in the literature. The experiments show that $O+O_2$ dissociation is approximately three times faster than O_2+O_2 dissociation. In this paper, we propose that these measurements provide the first experimental validation that DMS predictions of non-Boltzmann distributions are correct. Specifically, we show that this factor of three difference in measured rates is due to non-Boltzmann effects that strongly depend on the amount of atomic oxygen present.

2. DMS predictions compared to experimental measurement

2.1. Dissociation rates

Experiments performed in the shock-tube facility at Stanford university used absorption spectroscopy to infer dissociation rates in oxygen at various gas temperatures behind strong shock waves [27]. Similar experiments have been reported in the literature, however, the measurement uncertainty was too large to quantify differences between dissociation in $O+O_2$ systems compared to O_2+O_2 systems [28]. While the Stanford study compared the new measured data to a variety of CFD models, it did not compare to the DMS predictions published several years earlier. The purpose of this section is to compare the DMS predictions with this new, low-uncertainty, experimental data.

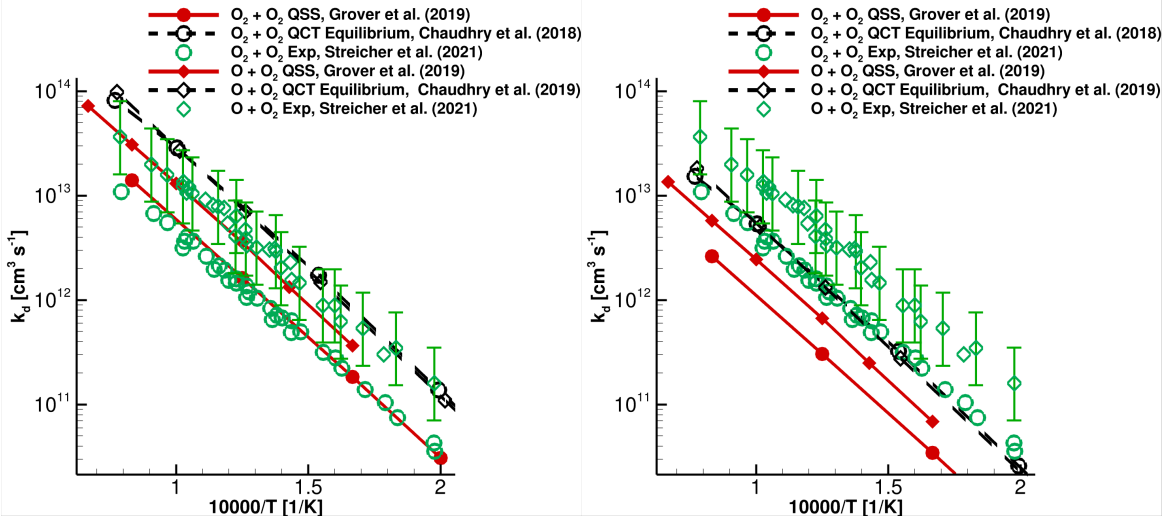

Fig 2. Experimental data for oxygen dissociation rates over a wide range of temperatures [27], compared with prior predictions from QCT [29] and DMS [16] calculations. (a) QCT and DMS including the 16/3 factor for electronic excitation, (b) Raw QCT and DMS results corresponding to ground electronic state interactions.

In Fig. 2, the Stanford experimental results are re-plotted (from Ref. 27) and compared to first-principles calculations using Quasi-Classical-Trajectory (QCT) analysis and DMS calculations, where both methods rely solely on the twelve required oxygen PESs developed by in the Department of Chemistry at the University of Minnesota [30-32]. The QCT and DMS results were published in 2018-2019 [29,16]; several years before the experiments. The first clear trend is that the QCT results show almost identical reaction rates for $O+O_2$ and O_2+O_2 collisions. In contrast, both the experimental data and DMS results show a consistent factor of 3 difference across a wide temperature range. Importantly, both QCT and DMS methods used the same PESs, the same trajectory integration source code, and the same post-processing source code. The only difference is that the QCT analysis sampled pre-collision internal energies from Boltzmann distributions at the specified temperature (hence labelled as "QCT-Equilibrium" in Fig. 2), whereas DMS simulations have no such restriction on the energy distribution functions, which evolve naturally during the simulation of a rapidly heated gas. The difference in dissociation rates is therefore due to non-Boltzmann effects, and indeed, the underlying vibrational energy distribution of O_2 particles in a DMS simulation containing mainly molecular oxygen differs noticeably from the distribution when significant atomic oxygen is present. This is explained in section 2.2.

An important caveat, is that the QCT and DMS dissociation rates shown in Fig. 2a have been multiplied by a constant factor of 16/3. The raw QCT and DMS results, without the factor, are shown in Fig. 1b. The reason results are plotted with and without this factor is to include upper and lower limits of the computed reaction rates due to electronically excited states of molecular oxygen that may be present in the experiments. Molecular oxygen has several excited electronic states that lie below the dissociation energy. If all of these electronic energy levels are fully populated in a QSS dissociating gas at temperature *T*, then the actual rate of dissociation could be higher than predicted by DMS simulations that include only ground electronic state molecules at the same *T*. As explained in detail in Ref. [16], the factor 16/3 results from summing the degeneracies of these electronic states and dividing by the degeneracy of the ground state as proposed by Nikitin [33]. By comparing Figs. 2a and 2b, the experimental data is best predicted by DMS results that include the full electronic excitation factor, which seems to indicate that these electronic states are populated under these conditions. However, this is not a rigorous conclusion and the *magnitude* of oxygen reaction rates could certainly vary between these two limits due to partial electronic excitation of O_2. However, the *difference* between reaction rates seen in the experiments (the factor of 3) is rigorously predicted by DMS simulations and is a result of non-Boltzmann vibrational energy distribution effects, as further described in the next section.

2.2. Non-Boltzmann Vibrational Energy Distributions

The vibrational energy distribution functions during the QSS reaction portion of isothermal DMS simulations are shown in Fig. 3a and 3b for heat bath temperatures of 6000 K and 10,000 K. These DMS simulations, and energy distributions, correspond to the same simulations where the dissociation rates were extracted and plotted in Fig. 2, and these results were previously reported in Ref. [16], and are only summarized here.

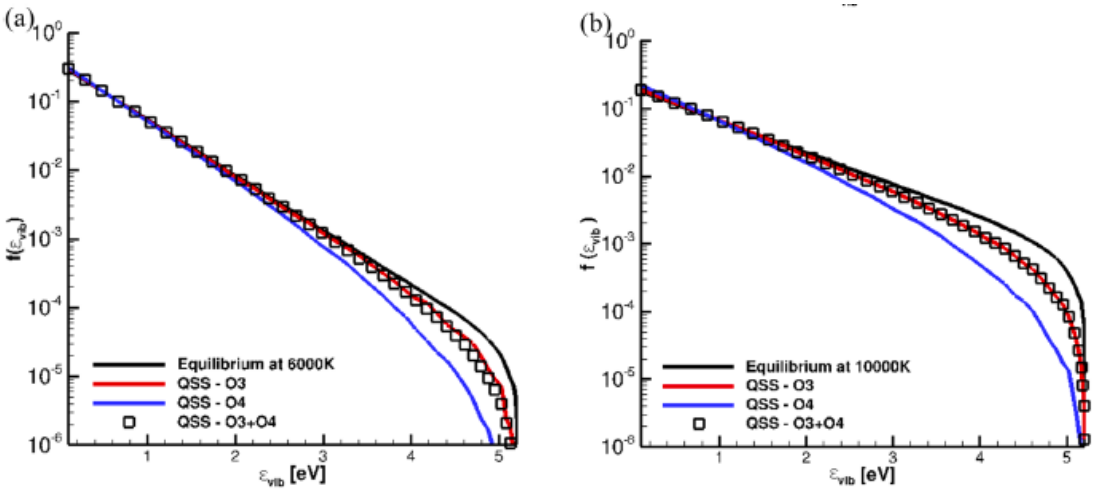

Fig. 3 Vibrational energy distributions in QSS predicted by DMS for isothermal heat baths at 6000 K and 10,000 K. Figure originally presented in Ref. [16].

As seen in Figs. 3a and 3b, the vibrational energy distribution during QSS for a DMS simulation where only O_2-O_2 collisions (O atoms are removed if they are created by dissociation) exhibits significant depletion of high energy states compared to the corresponding Boltzmann distribution at 6000 K. Since high energy molecules are exponentially more likely to dissociate, the lower population of high energy states results in a lower dissociation rate compared to that computed assuming a Boltzmann distribution (approximately 3 times lower as seen in Fig. 2). The degree of depletion is a competition between dissociation removing high vibrational energy states and inelastic collisions repopulating the high energy states. As quantified in Ref. [15], when O atoms are present, exchange collisions ($O^aO^b + O^c \rightarrow O^aO^c + O^b$) are highly probable. Such exchange collisions result in large, multi-quantum, changes in vibrational energy and therefore fast vibrational energy relaxation. As shown in Fig. 4 (taken from Ref. [16]) the vibrational relaxation time constant quantified by DMS simulations for a gas system involving only O_2-O_2 collisions is approximately 10 times higher (therefore slower relaxation) than for a gas system involving O-O_2 collisions. This trend is supported by limited experimental data also shown in Fig. 4. The QSS vibrational energy distribution predicted by DMS for a gas system involving O-O_2 collisions, shown in Figs. 3a and 3b show significantly less depletion compared to that found in the O_2-O_2 system. DMS calculations confirm this is a direct result of exchange collisions that rapidly repopulate the upper vibrational energy levels. This leads to a higher dissociation rate for the O-O_2 system compared to the O_2+O_2 system, yet still a lower dissociation rate than predicted assuming a Boltzmann distribution.

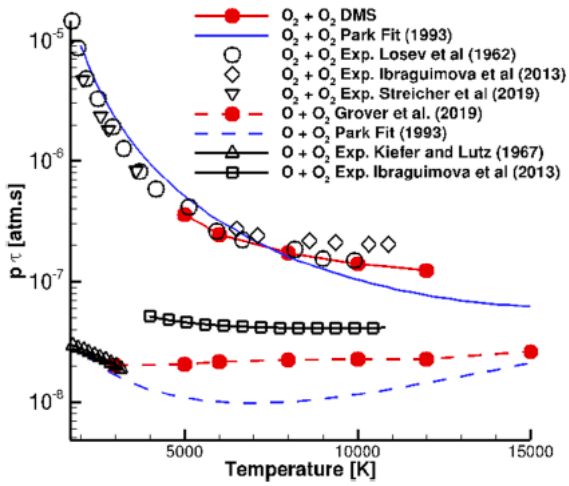

Fig. 4 Vibrational relaxation time constants (τ) predicted by DMS calculations for a range of temperature compared to time constants inferred from experiments. Figure originally presented in Ref. [16].

The concept of QSS depleted internal energy distributions is well established (for example refer to chapter 3 in Ref. [1]) and many studies have investigated QSS distribution functions and reaction rates [9-20]. However, as explained in the introduction, the DMS method is the only method capable of predicting rovibrational excitation and dissociation for both atom-diatom and diatom-diatom collisions without grouping or binning models. The DMS results in Figs. 2-4 are the only first-principles calculations that quantify and fully explain the factor of 3 difference in dissociation rates and have now been validated with low-uncertainty shock tube experiments (Fig. 2).

The same trends for internal energy coupling to chemistry were originally quantified by DMS for nitrogen flows [10]. However, experimental data with low quantified uncertainty are not available for nitrogen flows for validation these DMS results. As found for both nitrogen and oxygen systems, the difference in dissociation rates assuming Boltzmann distributions compared to the true QSS distributions from DMS (the "depletion factor") remains essentially constant across a wide temperature range, even at low temperatures where depletion is minimal. As detailed in Refs. [10] and [16], this is due to the fact that at low temperatures only molecules in the upper vibrational energy levels are able to dissociate and so even minimal depletion in their population results in a significant reduction in dissociation rate. Despite tight coupling between internal energy and dissociation chemistry, the resulting near-constant depletion factor is a fortunate result for modeling efforts.

2.3. Consistent QSS distributions for isothermal, adiabatic, and shock wave simulations

The results displayed in Figs. 2-4 were obtained by simulating isothermal heat bath conditions where the translational temperature was held constant by resampling the center-of-mass velocity of all particles after each timestep, while allowing particles' internal energies to evolve. After the gas system reaches a QSS dissociating phase, the distribution functions are sampled and reaction rates are extracted. While isothermal simulations are useful, it is possible that the internal energy and chemistry coupling effects observed are different than what occurs behind an actual shock wave.

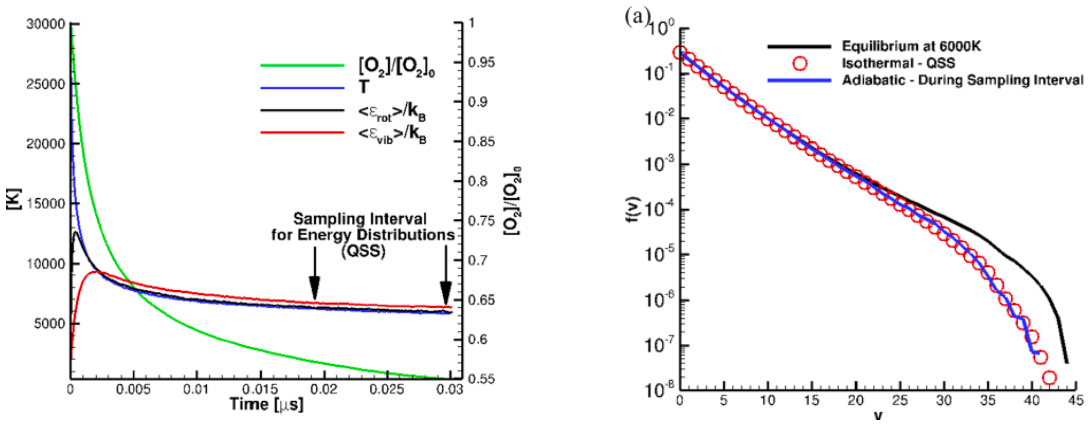

Fig. 5 Temperature and mole fraction histories for an adiabatic heat bath DMS simulation and the QSS vibrational energy distribution function. Figure originally presented in Ref. [16].

For this reason, DMS studies have been performed for adiabatic heat baths [13,16,17] and for normal shock wave simulations [8]. Figure 5 shows example DMS results (taken from Ref. [16]) for an adiabatic heat bath, where the initial translational temperature is high and initial rotational and vibrational temperatures are low, representative of conditions at just behind a strong shock-front. Such adiabatic simulations are more representative of post-shock conditions (compare with Fig. 1 for example). The translational, rotational, and vibrational energy modes relax towards each other while the gas dissociates. As indicated in Fig. 5a, the vibrational energy distribution function and dissociation rates are sampled during a specific QSS interval where the temperature is approximately 6000 K and the results are shown in Fig. 5b. As evident in Fig. 5b (and detailed in Ref. [16]), the depleted QSS vibrational energy distribution under adiabatic conditions is identical to the distribution under isothermal conditions at the same temperature. A further DMS study sampled vibrational energy distribution functions and dissociation probability density functions (pdfs) using normal shock simulations [8] (for example refer to Fig. 1). The vibrational energy distributions and dissociation pdfs sampled in the QSS region behind normal shocks were also found to agree with the results from adiabatic and isothermal calculations. Therefore, DMS calculations have convincingly shown that depleted vibrational energy populations are expected to persist in the post-shock QSS region; precisely where experimental measurements are most often made. Therefore, simulations (such as DMS) that resolve the underlying non-Boltzmann energy distributions and their coupling to dissociation better predict the difference in dissociation rates between O_2-O_2 and O-O_2 systems, compared to assuming Boltzmann energy distributions (the QCT-Equilibrium results), as shown in Fig. 2.

A model for non-Boltzmann internal energy distribution functions that includes both overpopulation and depletion effects has been developed by Singh and Schwartzentruber [34-36] using surprisal analysis combined with DMS results. The model has even been extended to include repopulation of high internal energy states due to recombination [36]. Given the local gas state including average internal energy content (T, Tr, and Tv) an analytical expression is able to capture the non-Boltzmann aspects of internal energy distributions during rapid excitation and QSS phases and limits to the Boltzmann distribution for chemical equilibrium. This model has been incorporated into a new multi-temperature model that now explicitly accounts for non-Boltzmann effects [37,38]. Additionally, the model for non-Boltzmann internal energy distributions [36] may be useful as a post-processing tool for CFD solutions, where it provides an estimate of the energy populations at each point in the flowfield (given the local T, Tr, and Tv). This information could be useful for researchers studying radiative emission in high-speed flows.

Finally, it is also possible that for dissociating 5-species air that Zeldovich exchange reactions (for example N_2+O ↔ NO+N and O_2+N ↔ NO+O act to rapidly relax vibrational energy of the molecular species that could result in minimal depletion effects (near-Boltzmann energy distributions). However, recent DMS calculations have been performed for 5-species air and results show depleted vibrational energy distributions for each diatomic species (O_2, N_2, and NO) in the mixture [25]. DMS and QCT studies for 5-species air are ongoing and will provide a full picture of rovibrational excitation and dissociation for high-speed air flow.

4. Conclusions

Reaction rate coefficients, inferred from recent shock tube experiments with low measurement uncertainty, are directly compared to predictions from first-principles simulations that were published several years before the experiments. Both the experimental data and the first-principles simulations indicate that oxygen dissociation proceeds approximately three times faster when significant oxygen atoms are present (mainly O-O_2 collisions), compared to a gas comprised mainly of molecular oxygen (where O_2-O_2 collisions dominate).

Specifically, prior direct molecular simulation (DMS) calculations [16] of dissociating gas mixtures are summarized that included *both* atom-diatom and diatom-diatom collision dynamics. It was found that O_2 dissociation occurs three times faster in the presence of significant atomic oxygen (O), compared to O_2 dissociation in a gas comprised mainly of O_2. DMS and QCT calculations clearly show that this difference is *not* because O atoms are more efficient at dissociating an O_2 molecule compared to dissociation via O_2+O_2 collisions, on a per-collision basis. Rather, DMS calculations show this is an indirect result of rapid vibrational energy excitation (approximately ten times higher) promoted by O+O_2 exchange collisions, which increase the population of upper vibrational states of O_2 molecules in the gas leading to faster dissociation [16]. Similar DMS predictions of non-Boltzmann vibrational energy populations and coupling to dissociation were made for nitrogen mixtures [10].

Although the analysis is for oxygen in the ground electronic state, non-Boltzmann rovibrational energy distributions and coupling to dissociation appears to fully account for the difference in reaction rates observed experimentally. Further effort is required to understand what effect electronic energy excitation has on this trend in dissociation rates (if any). Currently PESs are being constructed including electronically excited states of oxygen and the couplings between surfaces using deep neural network methos methods [39].

In summary, the new experimental measurements are remarkably consistent with the prior DMS predictions and, for the first time, validate predictions of non-Boltzmann internal energy populations behind strong shock waves and their coupling to dissociation.

References

1. Park, C., Nonequilibrium hypersonic aerothermodynamics, Wiley, New York, 1990.
2. Candler, G. V., "Rate Effects in Hypersonic Flows," Annual Review of Fluid Mechanics, Vol. 51, No. 1, 2019, pp. 379–402.
3. Park, C., "Two-Temperature Interpretation of Dissociation Rate Data for N2 and O2," 26th Aerospace Sciences Meeting, AIAA Paper 1988-458, 1988.
4. Marrone, P. V., and Treanor, C. E., "Chemical Relaxation with Preferential Dissociation from Excited Vibrational Levels," The Physics of Fluids, Vol. 6, No. 9, 1963, pp. 1215–1221.
5. Chaudhry, R.S., Boyd, I.D., Torres, E., Schwartzentruber, T.E., and Candler, G.V., "Implementation of a Chemical Kinetics Model for Hypersonic Flows in Air for High-Performance CFD", AIAA Paper 2020-1715, presented at the AIAA SciTech Forum, Orlando, FL.
6. Chaudhry, R.S., Boyd, I.D., and Candler, G.V., "Vehicle-Scale Simulations of Hypersonic Flows using the MMT Chemical Kinetics Model", AIAA Paper 2020-3272, presented at the AIAA Aviation Forum.
7. Hornung, H. "Induction time for nitrogen dissociation," J. Chem. Phys., Vol. 56, pp. 3172–3173 (1972).
8. Torres, E. and Schwartzentruber, T.E., 2022, "Direct molecular simulation of oxygen dissociation across normal shocks", Theoretical and Computational Fluid Dynamics, 36(1), pp.41-80.

9. Valentini, P., Schwartzentruber, T., Bender, J., Nompelis, I., and Candler, G., "Direct molecular simulation of nitrogen dissociation based on an ab initio potential energy surface," Physics of Fluids, Vol. 27, 2015, p. 086102.
10. Valentini, P., and Schwartzentruber, T., "Direct molecular simulation of high-temperature nitrogen dissociation due to both N-N2 and N2-N2 collisions," 45th AIAA Thermophysics Conference, Dallas, TX, 2015. AIAA 2015-3254.
11. Jaffe, R., Grover, M., Venturi, S., Schwenke, D., Valentini, P., Schwartzentruber, T., and Panesi, M., "Comparison of Potential Energy Surface and Computed Rate Coefficients for N2 Dissociation," Journal of Thermophysics and Heat Transfer, Vol. 32, No. 4, 2018, pp. 869–881.
12. Macdonald, R., Grover, M., Schwartzentruber, T., and Panesi, M., "Construction of a coarse-grain quasi-classical trajectory method. II. Comparison against the direct molecular simulation method," The Journal of Chemical Physics, Vol. 148, No. 5, 2018, p. 054310.
13. Torres, E., and Schwartzentruber, T., "Direct molecular simulation of nitrogen dissociation under adiabatic post-shock conditions," Journal of Thermophysics and Heat transfer, Vol. 34, No. 4, 2020, pp. 801–815. doi:10.2514/1.T5970, URL https://doi.org/10.2514/1.T5970.
14. Macdonald, R., Torres, E., Schwartzentruber, T., and Panesi, M., "State-to-State Master Equation and Direct Molecular Simulation Study of Energy Transfer and Dissociation for the N2 − N System," The Journal of Physical Chemistry A, 2020. doi:10.1021/acs.jpca.0c04029.
15. Grover, M., Schwartzentruber, T., Varga, Z., and Truhlar, D., "Vibrational Energy Transfer and Collision-Induced Dissociation in O + O2 Collisions," Journal of Thermophysics and Heat Transfer, Vol. 33, No. 3, 2019, pp. 797–807.
16. Grover, M., Torres, E., and Schwartzentruber, T., "Direct molecular simulation of internal energy relaxation and dissociation in oxygen," Physics of Fluids, Vol. 31, 2019, p. 076107.
17. Torres, E., and Schwartzentruber, T., "Direct molecular simulation of dissociating oxygen under adiabatic and normal shock wave conditions," AIAA Scitech 2021 Forum, 2021.
18. Kim, J., and Boyd, I., "State-resolved master equation analysis of thermochemical nonequilibrium of nitrogen," Chemical Physics, Vol. 415, 2013, pp. 237–246.
19. Panesi,M., Jaffe, R., Schwenke, D., andMagin, T., "Rovibrational internal energy transfer and dissociation of N2−N system in hypersonic flows," The Journal of Chemical Physics, Vol. 138 (4), 2013, p. 044312
20. Armenise, I., and Esposito, F., "N2, O2, NO ate-to-ate vibrational kinetics in hypersonic boundary layers: The problem of rescaling rate coefficients to uniform vibrational ladders," Chemical Physics, Vol. 446, 2015, p. 30–46. doi:10.1016/j.chemphys.2014.11.004.
21. Norman, P., Valentini, P., and Schwartzentruber, T., "GPU-Accelerated Classical Trajectory Calculation Direct Simulation Monte Carlo Applied to Shock Waves," Journal of Computational Physics, Vol. 247, 2013, pp. 153–167.
22. Schwartzentruber, T.E., Grover, M., and Valentini, P., "Direct Molecular Simulation of Nonequilibrium Dilute Gases", *Journal of Thermophysics and Heat Transfer*, Vol. 32, No. 4, pp. 892-903 (2018).
23. Koura, K., "Monte Carlo direct simulation of rotational relaxation of diatomic molecules using classical trajectory calculations: Nitrogen shock wave," Physics of Fluids, Vol. 9, 1997, p. 3543.
24. Valentini, P., Grover, M.S., Bisek, N. and Verhoff, A., 2021. Molecular simulation of flows in thermochemical non-equilibrium around a cylinder using ab initio potential energy surfaces for N2+ N and N2+ N2 interactions. Physics of Fluids, 33(9), p.096108.
25. Torres, E., T. Gross, E. Geistfeld, and T.E. Schwartzentruber. "Verification of nonequilibrium thermochemistry models for hypersonic CFD by first-principles simulation.", Eleventh International Conference on Computational Fluid Dynamics 2022, ICCFD11-2022-2201.

26. Duchovic, R., Volobuev, Y., Lynch, G., Jasper, A., Truhlar, D., Allison, T., Wagner, A., Garrett, B., Espinosa García, J., and Corchado, J., "POTLIB library," http://comp.chem.umn.edu/potlib

27. Streicher, J., Krish, A., and Hanson, R., "Coupled vibration-dissociation time-histories and rate measurements in shockheated, nondilute O2 and O2 – Ar mixtures from 6000 to 14000 K," Physics of Fluids, Vol. 33, No. 5, 2021, pp. 056107.

28. Ibraguimova, L., Sergievskaya, A., Levashov, V., Shatalov, O., Tunik, Y., and Zabelinskii, I., "Investigation of oxygen dissociation and vibrational relaxation at temperatures 4000-10800 K," The Journal of Chemical Physics, No. 139, 2013, p.034317.

29. R. S. Chaudhry and G. V. Candler, "Statistical analyses of quasiclassical trajectory data for air dissociation," in AIAA SciTech 2019 Forum, AIAA paper 2019-0789.

30. Paukku, K. R. Yang, Z. Varga, G. Song, J. D. Bender, and D. G. Truhlar, "Potential energy surfaces of quintet and singlet O4," J. Chem. Phys. 147, 034301 (2017).

31. Paukku, Z. Varga, and D. G. Truhlar, "Potential energy surface of triplet O4," J. Chem. Phys. 148, 124314 (2018).

32. Varga, Y. Paukku, and D. G. Truhlar, "Potential energy surfaces for O + O2 collisions," J. Chem. Phys. 147, 154312 (2017).

33. E. Nikitin, Theory of Elementary Atomic and Molecular Processes in Gases (Clarendon Press, Oxford, 1974).

34. Singh, N. and Schwartzentruber, T.E., "Non-Equilibrium Internal Energy Distributions During Dissociation", Proceedings of the National Academy of Sciences, Vol. 115, No. 1, pp. 47-52 (2018).

35. Singh, N. and Schwartzentruber, T.E., "Non-Boltzmann Vibrational Energy Distributions and Coupling to Dissociation Rate", Journal of Chemical Physics, 152, 224301 (2020).

36. Singh, N. and Schwartzentruber, T.E., "Nonequilibrium Dissociation and Recombination in Hypersonic Flows", AIAA Journal (2022), 60(5), pp. 2810-2825.

37. Singh, N. and Schwartzentruber, T.E., "Consistent Kinetic-Continuum Dissociation Model I: Kinetic Formulation", Journal of Chemical Physics, 152, 224302 (2020).

38. Singh, N. and Schwartzentruber, T.E., "Consistent Kinetic-Continuum Dissociation Model II: Continuum Formulation and Verification", Journal of Chemical Physics, 152, 224303 (2020).

39. Shu, Varga, Oliveira-Filho, Truhlar, Permutationally Restrained Diabatization by Machine Intelligence, JCTC 17(2) 2021, pp. 1106-1116.